Baek et al. Nanoscale Research Letters (2015) 10:388
DOI 10.1186/s11671-015-1094-x

Nanoscale Research Letters
a SpringerOpen Journal

NANO EXPRESS Open Access

Large-Area Growth of Uniform Single-Layer MoS_2 Thin Films by Chemical Vapor Deposition

Seung Hyun Baek, Yura Choi and Woong Choi*

Abstract

We report the largest-size thin films of uniform single-layer MoS_2 on sapphire substrates grown by chemical vapor deposition based on the reaction of gaseous MoO_3 and S evaporated from solid sources. The as-grown thin films of single-layer MoS_2 were continuous and uniform in thickness for more than 4 cm without the existence of triangular-shaped MoS_2 clusters. Compared to mechanically exfoliated crystals, the as-grown single-layer MoS_2 thin films possessed consistent chemical valence states and crystal structure along with strong photoluminescence emission and optical absorbance at high energy. These results demonstrate that it is possible to scale up the growth of uniform single-layer MoS_2 thin films, providing potentially important implications on realizing high-performance MoS_2 devices.

Keywords: MoS_2; Single layer; Thin films; Chemical vapor deposition

PACS: 81.05.Hd; 81.10.Bk; 81.15.Gh

Background

Two-dimensional transition metal dichalcogenides (TMDs) have received great attention because of their interesting electronic, optical, and chemical properties. Among various TMDs, molybdenum disulfide (MoS_2) has been most extensively investigated for the applications of thin-film transistors (TFTs), photodetectors, and energy storage [1–3]. TFTs based on single- or multilayer MoS_2 exhibit intriguing transistor performance including high on/off current ratio (~10^7), high mobility at room temperature (~100 cm^2 V^{-1} s^{-1}), and low subthreshold swing (~70 mV $decade^{-1}$) [4, 5]. Moreover, photodetectors based on single- or multilayer MoS_2 show high photoresponsivity (300–800 A W^{-1}) exceeding that of silicon-based ones [6, 7]. However, the aforementioned examples have been demonstrated using mechanically exfoliated MoS_2 flakes, which are typically micrometer-scale in size. Hence, the growth of large-area MoS_2 is one of the critical challenges to realize its promising potential.

So far, a variety of synthesis approaches have been reported to grow large-area MoS_2 including liquid exfoliation (sonication in solvents) [8], two-step chemical vapor deposition (CVD, sulfurization or decomposition of pre-deposited Mo-based thin films) [9–11], one-step CVD (reaction of gaseous Mo and S precursors) [12–14], and physical vapor deposition (sputtering and pulsed laser deposition) [15, 16]. Special emphasis has been put on one-step CVD as it shows greater potential for growing uniform large-grain thin films of single-layer MoS_2. The most common one-step CVD is based on the reaction of gaseous MoO_3 and S evaporated from solid sources due to the simplicity of processing and the easy availability of solid sources [12]. When the optimized CVD process conditions with MoO_3 and S precursors are combined with the use of mica or substrate treatment, the formation of single-layer MoS_2 thin films can be obtained up to about a centimeter [17–19]. However, CVD processes based on MoO_3 and S powders typically result in triangular-shaped discontinuous clusters of either single-layer MoS_2 or mixtures of single- and few-layer MoS_2 [12]. Therefore, more work is needed to establish a CVD process that can reproducibly provide continuous large-area thin films of uniform single-layer MoS_2.

* Correspondence: woongchoi@kookmin.ac.kr
School of Advanced Materials Engineering, Kookmin University, Seoul 02707, South Korea

Here, we investigate CVD methods based on MoO_3 and S powders to grow continuous thin films of single-layer MoS_2 for more than 4 cm on sapphire substrates. Our MoS_2 thin films are the largest in size grown by CVD methods based on MoO_3 and S powders. The large-area deposition, thickness uniformity, and crystallinity of single-layer MoS_2 thin films are confirmed by scanning electron microscopy (SEM), atomic force microscopy (AFM), x-ray photoelectron spectroscopy (XPS), Raman spectroscopy, photoluminescence (PL) spectroscopy, ultraviolet (UV)-visible spectroscopy, and transmission electron microscopy (TEM).

Methods

MoS_2 films were deposited on (0001)-oriented sapphire substrates in a two-zone tube furnace. MoO_3 (99.98 %, Sigma-Aldrich) and S (99.98 %, Sigma-Aldrich) powders in two separate Al_2O_3 boats were used as precursors. MoO_3 powder (15 mg) was placed upstream at zone 1 (700 °C), and S powder (1 g) was placed at the upstream entry of the furnace. The substrates were placed downstream at zone 2 (600 °C). MoO_3 powder was heated up to 700 °C at a rate of 15 °C min^{-1}, and the substrates were heated up to 600 °C at 38 °C min^{-1}. After 30-min deposition, the furnace was slowly cooled down to room temperature. Ar flow of 100 sccm and a pressure of ~0.5 Torr were maintained during deposition.

The surface morphology of deposited thin films was observed by SEM (JEOL JSM-7610F) and AFM (Park Systems XE-100). Elemental composition was analyzed using XPS (PHI X-tool). The thickness and uniformity of deposited thin films were measured by Raman and PL spectra (Horiba LabRAM Aramis) using a laser of 532 nm in wavelength. Optical

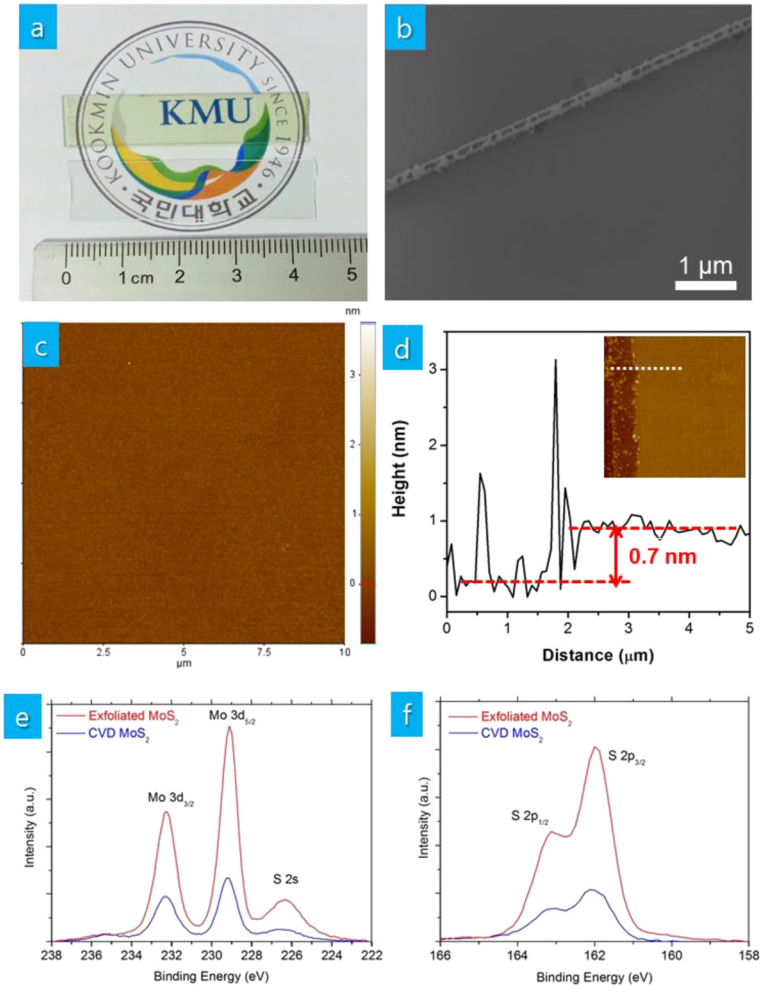

Fig. 1 **a** As-grown MoS_2 thin films on a sapphire substrate in comparison with a bare sapphire substrate, **b** SEM image of an intentionally scratched MoS_2 thin films, **c** AFM image, **d** cross-sectional AFM image along the dotted line in the AFM image, **e**, **f** XPS spectra of MoS_2 thin films along with those of mechanically exfoliated MoS_2 flakes

absorbance was measured by UV-visible spectroscopy (PerkinElmer Lambda 35). Crystal structure was analyzed by TEM (FEI Titan 80–300) at 300 kV.

Results and Discussion

MoS_2 thin films deposited on sapphire substrates are light yellow-green in color exhibiting obvious color contrast with transparent bare sapphire substrates as shown in Fig. 1a. The continuous formation of MoS_2 thin films is observed up to 4 cm. The existence of MoS_2 thin films on substrates can be confirmed by the color contrast in the SEM image of an intentionally scratched sample in Fig. 1b. When MoO_3 and S powders are used as precursors, triangular-shaped discontinuous clusters of either single-layer MoS_2 or mixtures of single- and few-layer MoS_2 are typically observed in literature [12]. Similarly, triangular-shaped clusters or regions of bilayer MoS_2 can be observed in this investigation when process conditions are not optimized (see Additional file 1). However, with optimized process conditions, such triangular clusters of MoS_2 cannot be found in our MoS_2 thin films as shown Fig. 1b. The absence of triangular clusters of MoS_2 is further confirmed by AFM image in Fig. 1c. The AFM measurement on the scratched sample in Fig. 1d shows thickness of 0.7 nm corresponding to that of single-layer MoS_2. As MoS_2 growth is known to be sensitive to the localized concentration of precursors [20], the combination of the low pressure, distance between precursors and substrates, and temperature used in this investigation may result in uniform nucleation and growth of MoS_2. Figure 1e, f compares XPS of the deposited MoS_2 thin films with that of bulk MoS_2 single crystals. The existence of Mo^{4+} (Mo $3d_{5/2}$ orbital at 229.1 eV and Mo $3d_{3/2}$ orbital at 232.3 eV) and S^{2-} (S $2p_{3/2}$ orbital at 162.0 eV and S $2p_{1/2}$ orbital at 163.1 eV) is clearly seen in our thin films.

To confirm the thickness of deposited MoS_2 thin films, we measure the Raman spectra of deposited MoS_2 thin films. Figure 2a shows the two characteristic Raman A_{1g} and E^1_{2g} modes of four different MoS_2 samples—CVD MoS_2 thin films on sapphire substrates, CVD MoS_2 thin films transferred on SiO_2/Si substrates, mechanically exfoliated single-layer MoS_2 flakes on SiO_2/Si substrates, and bulk MoS_2 single crystals. The frequency difference between A_{1g} and E^1_{2g} modes (Δ) of MoS_2 is related to its thickness [21]. Except bulk single crystals ($\Delta = 25.1\ cm^{-1}$), all other MoS_2 samples possess Δ between 19.6 and 19.9 cm^{-1} suggesting single-layer MoS_2. It needs to be mentioned that the positions of A_{1g} and E^1_{2g} modes are slightly shifted for single-layer MoS_2 on SiO_2/Si substrates (both transferred CVD films and mechanically exfoliated MoS_2 flakes). This is due to the effect of underlying SiO_2/Si substrates as substrates can strongly affect the Raman and PL emission of single-layer MoS_2 [22].

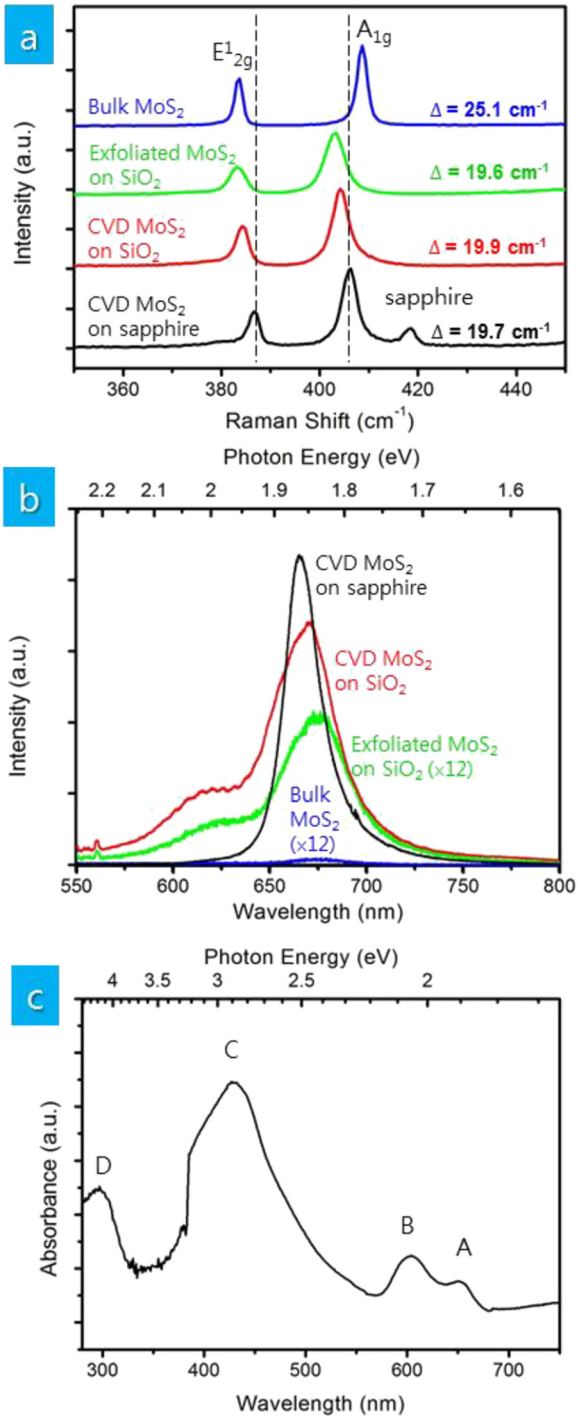

Fig. 2 **a** Raman and **b** PL spectra of MoS_2 thin films on sapphire and SiO_2/Si, mechanically exfoliated MoS_2 flakes on SiO_2/Si, and bulk MoS_2 crystals and **c** UV-visible spectrum of MoS_2 thin films on sapphire

The thickness of MoS_2 thin films is further confirmed by PL spectra. While the indirect bandgap of multilayer MoS_2 does not allow PL emission, the direct bandgap of

single-layer MoS_2 allows PL emission [23, 24]. Figure 2b shows the PL spectra of the same four MoS_2 samples—CVD MoS_2 thin films on sapphire substrates, CVD MoS_2 thin films transferred on SiO_2/Si substrates, mechanically exfoliated single-layer MoS_2 flakes on SiO_2/Si substrates, and bulk MoS_2 single crystals. While the emission intensity completely disappears for bulk MoS_2, our single-layer MoS_2 thin films on sapphire show a PL emission peak at 1.88 eV confirming they are single-layer MoS_2. The PL spectrum of our single-layer MoS_2 thin films on sapphire is different from that of mechanically exfoliated single-layer MoS_2 flakes on SiO_2/Si. Two emission peaks are observed for mechanically exfoliated single-layer MoS_2 flakes on SiO_2/Si at 1.85 and 2.00 eV known as A and B direct excitonic transitions [23, 24]. The shift of emission peak A and the absence of emission peak B in our single-layer MoS_2 thin films on sapphire are due to the effect of the underlying substrate [22]. The consistent PL emission spectrum from transferred single-layer MoS_2 on SiO_2/Si with that of mechanically exfoliated single-layer MoS_2 flakes on SiO_2/Si supports this.

The UV-visible absorption spectrum in Fig. 2c shows A and B absorption due to excitonic transitions along with C and D absorption associated with van Hove singularity [25, 26]. As the existence of van Hove singularity can enhance light-matter interactions, single-layer MoS_2 thin films may be suitable for photovoltaic cells and photodetectors due to enhanced photon absorption and electron-hole creation.

We also perform TEM analysis to obtain information on the crystallinity of the single-layer MoS_2 thin films. The low-magnification bright-field TEM cross-sectional image in Fig. 3a shows continuous single-layer MoS_2 thin films on sapphire substrates. The high-resolution plan-view image in Fig. 3b and the corresponding fast Fourier transformation pattern in its inset reveal the hexagonal crystal structure of single-layer MoS_2 thin films. The estimated interplanar spacing of (100) and (110) planes is ~0.28 and ~0.16 nm, respectively, which is in good agreement with literature [12]. The selected area electron diffraction (SAED) pattern obtained from the low-magnification plan-view image in Fig. 3c shows multiple rings confirming the polycrystalline nature of the MoS_2 thin films.

For more quantitative assessment of the thickness uniformity, Raman and PL spectra are measured at eight different positions of a 4-cm-wide single-layer MoS_2 thin film (insets of Fig. 4a, b). Figure 4a, b shows negligible variation of the measured full-width at half maximum (FWHM) of Raman A_{1g} and E^1_{2g} modes, Δ, FWHM of PL emission peak, and PL emission wavelength. Figure 4c, d

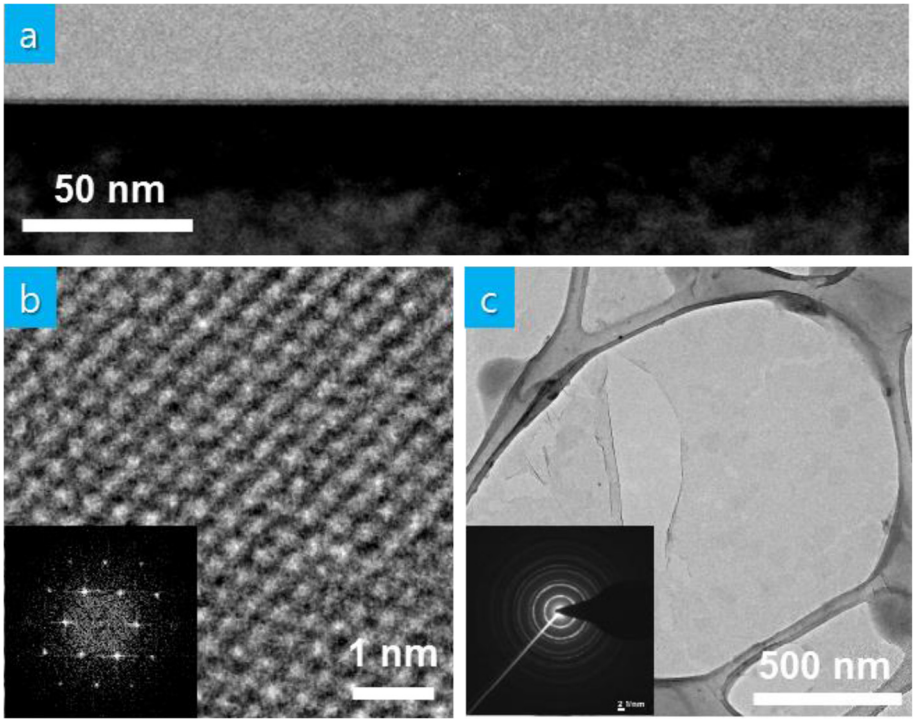

Fig. 3 **a** Cross-sectional TEM image of MoS_2 thin films on sapphire, **b** high-magnification plan-view TEM image along with fast Fourier transformation pattern, **c** low-magnification plan-view TEM image along with SAED pattern MoS_2 thin films

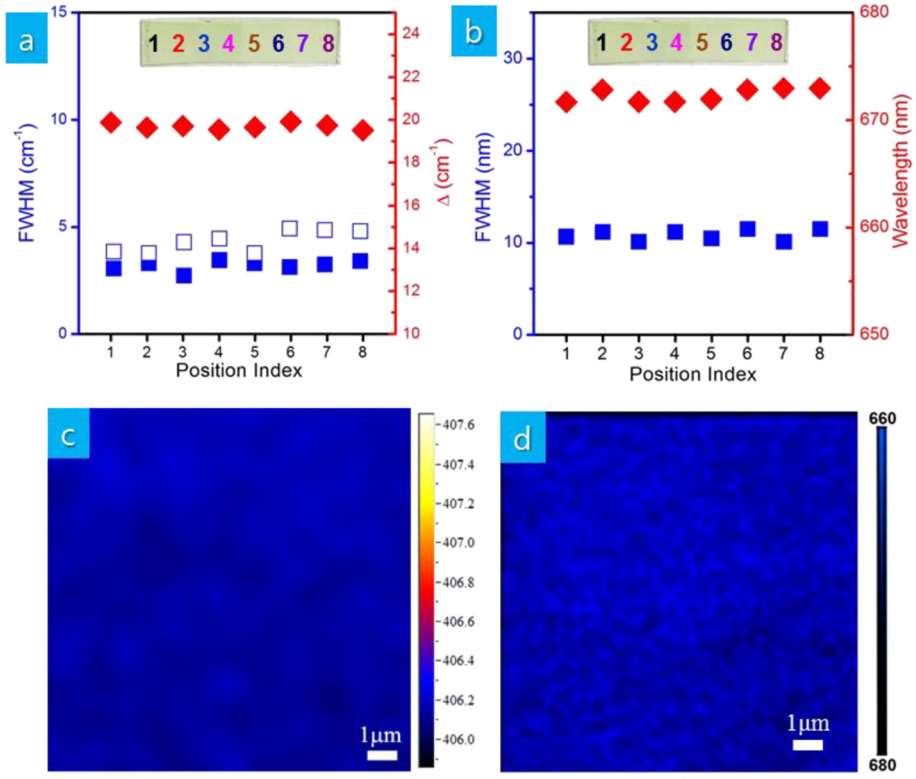

Fig. 4 **a** FWHM of Raman E^1_{2g} and A_{1g} modes along with Δ (red diamond: Δ, white square: FWHM of Raman A_{1g} mode, blue square: FWHM of Raman E^1_{2g} mode) and **b** FWHM along with wavelength of PL emission (red diamond: wavelength of PL emission, blue square: FWHM of PL emission) measured at eight different positions of MoS_2 thin films shown in the inset, **c** mapping of Raman A_{1g} mode frequency, and **d** mapping of PL emission wavelength of MoS_2 thin films

shows the measured Raman A_{1g} mode frequency and PL emission wavelength based on mapping over an area of 10 μm × 10 μm, respectively. Measured Raman A_{1g} mode frequency and PL emission wavelength exist in a range of 406.1–406.3 cm^{-1} and 659–662 nm, respectively. These results suggest that the thickness of our single-layer MoS_2 thin films is uniform across the substrate.

Conclusions

In summary, we synthesized uniform large-area thin films of single-layer MoS_2 on sapphire substrates by CVD based on MoO_3 and S precursors. The as-grown thin films were composed of single-layer MoS_2 and continuous for more than 4 cm without triangular-shaped clusters of MoS_2. The chemical configuration, thickness, thickness uniformity, and crystalline quality of MoS_2 thin films were confirmed by XPS, AFM, Raman and PL spectra, and TEM analysis. The optical absorbance measurement further suggested the existence of van Hove singularity at high energy. These results will help scale up the growth of two-dimensional TMDs, providing potentially important implications on realizing the promising potential of high-performance MoS_2 devices such as thin-film transistors, sensors, and photodetectors.

Additional file

Additional file 1: Formation of nonuniform MoS_2 clusters.
(DOCX 379 kb)

Competing Interests

The authors declare that they have no competing interests.

Authors' Contributions

SB and WC initiated the research and analyzed experimental data. SB worked on the growth and characterization of CVD thin films. YC worked on the fabrication and characterization of mechanically exfoliated single-layer flakes. WC wrote the manuscript. All authors read and approved the final manuscript.

Acknowledgments

This work was supported by the National Research Foundation of Korea (Grant NRF-2013R1A1A2008191, NRF-2013K1A4A3055679, and NRF-2013K1A3A1A32035549) and Industrial Strategic Technology Development Program (Grant 10045145).

Received: 17 August 2015 Accepted: 27 September 2015
Published online: 06 October 2015

References

1. Lembke D, Bertolazzi S, Kis A (2015) Single-layer MoS_2 electronics. Acc Chem Res 48:100–110
2. Xia F, Wang H, Xiao D, Dubey M, Ramasubramaniam A (2014) Two-dimensional material nanophotonics. Nat Photon 8:899–907

3. Bonaccorso F, Colombo L, Yu G, Stoller M, Tozzini V, Ferrari AC, Ruoff RS, Pellegrini V (2015) Graphene, related two-dimensional crystals, and hybrid systems for energy conversion and storage. Science 347:1246501
4. Radisavljevic B, Radenovic A, Brivio J, Giacometti V, Kis A (2011) Single-layer MoS_2 transistors. Nat Nanotechnol 6:147–50
5. Kim S, Konar A, Hwang WS, Lee JH, Lee J, Yang J, Jung C, Kim H, Yoo JB, Choi JY, Jin YW, Lee SY, Jena D, Choi W, Kim K (2012) High-mobility and low-power thin-film transistors based on multilayer MoS_2 crystals. Nat Commun 3:1011
6. Lopez-Sanchez O, Lembke D, Kayci M, Radenovic A, Kis A (2013) Ultrasensitive photodetectors based on monolayer MoS_2. Nat Nanotech 8:497–501
7. Kwon J, Hong YK, Han G, Omkaram I, Choi W, Kim S, Yoon Y (2015) Giant photoamplification in indirect-bandgap multilayer MoS_2 phototransistors with local bottom-gate structures. Adv Mater 27:2224–30
8. Coleman JN, Lotya M, O'Neill A, Bergin SD, King PJ, Khan U, Young K, Gaucher A, De S, Smith RJ, Shvets IV, Arora SK, Stanton G, Kim H-Y, Lee K, Kim GT, Duesberg GS, Hallam T, Boland JJ, Wang JJ, Donegan JF, Grunlan JC, Moriarty G, Shmeliov A, Nicholls RJ, Perkins JM, Grieveson EM, Theuwissen K, McComb DW, Nellist PD, Nicolosi V (2011) Two-dimensional nanosheets produced by liquid exfoliation of layered materials. Science 331:568–71
9. Liu KK, Zhang W, Lee Y-H, Lin Y-C, Chang M-T, Su C-Y, Chang C-S, Li H, Shi Y, Zhang H, Lai C-S, Li L-J (2012) Growth of large-area and highly crystalline MoS_2 thin layers on insulating substrates. Nano Lett 12:1538–44
10. Zhan Y, Liu Z, Najmaei S, Ajayan PM, Lou J (2012) Large-area vapor-phase growth and characterization of MoS_2 atomic layers on a SiO_2 Substrate. Small 8:966–71
11. Lin Y-C, Zhang W, Huang J-K, Liu K-K, Lee Y-H, Liang C-T, Chu C-W, Li L-J (2012) Wafer-scale MoS_2 thin layers prepared by MoO_3 sulfurization. Nanoscale 4:6637–41
12. Lee Y-H, Zhang X-Q, Zhang W, Chang M-T, Lin C-T, Chang K-D, Yu Y-C, Wang JT-W, Chang C-S, Li L-J, Lin T-W (2012) Synthesis of large-area MoS_2 atomic layers with chemical vapor deposition. Adv Mater 24:2320–25
13. Yu Y, Li C, Liu Y, Su L, Zhang Y, Cao L (2013) Controlled scalable synthesis of uniform, high-quality monolayer and few-layer MoS_2 films. Sci Rep 3:1866
14. Kang K, Xie S, Huang L, Han Y, Huang PY, Mak KF, Kim C-J, Muller D, Park J (2015) High-mobility three-atom-thick semiconducting films with wafer-scale homogeneity. Nature 520:656–60
15. Serrao CR, Diamond AM, Hsu S-L, You L, Gadgil S, Clarkson J, Carraro C, Maboudian R, Hu C, Salahuddin S (2015) Highly crystalline MoS_2 thin films grown by pulsed laser deposition. Appl Phys Lett 106:052101
16. Ling ZP, Yang R, Chai JW, Wang SJ, Leong WS, Tong Y, Lei D, Zhou Q, Gong X, Chi DZ, Ang K-W (2015) Large-scale two-dimensional MoS_2 photodetectors by magnetron sputtering. Opt Exp 23:13580–86
17. Ji Q, Zhang Y, Gao T, Zhang Y, Ma D, Liu M, Chen Y, Qiao X, Tan P-H, Kan M, Feng J, Sun Q, Liu Z (2013) Epitaxial monolayer MoS_2 on mica with novel photoluminescence. Nano Lett 13:3870–77
18. Dumcenco D, Ovchinnikov D, Marinov K, Lazic P, Gibertini M, Marzari N, Lopez-Sanchez O, Kung Y-C, Krasnozhon D, Chen M-W, Bertolazzi S, Gillet P, Fontcuberta i Morral A, Radenovic A, Kis A (2015) Large-area epitaxial monolayer MoS_2. ACS Nano 9:4611–20
19. Jeon J, Jang SK, Jeon SM, Yoo G, Jang YH, Park J-H, Lee S (2015) Layer-controlled CVD growth of large-area two-dimensional MoS_2 films. Nanoscale 7:1688–95
20. Ji Q, Zhang Y, Zhang Y, Liu Z (2015) Chemical vapour deposition of group-VIB metal dichalcogenide monolayers: engineered substrates from amorphous to single crystalline. Chem Soc Rev 44:2587–602
21. Lee C, Yan H, Brus LE, Heinz TF, Hone J, Ryu S (2010) Anomalous lattice vibrations of single and few-layer MoS_2. ACS Nano 4:2695–700
22. Buscema M, Steele GA, van der Zant HSJ, Castellanos-Gomez A (2014) The effect of the substrate on the Raman and photoluminescence emission of single-layer MoS_2. Nano Res 7:561–71
23. Splendiani A, Sun L, Zhang Y, Li T, Kim J, Chim C, Galli G, Wang F (2010) Emerging photoluminescence in monolayer MoS_2. Nano Lett 10:1271–5
24. Mak KF, Lee C, Hone J, Shan J, Heinz TF (2010) Atomically thin MoS_2: a new direct-gap semiconductor. Phys Rev Lett 105:136805
25. Britnell L, Ribeiro RM, Eckmann A, Jalil R, Belle BD, Mishchenko A, Kim Y-J, Gorbachev RV, Georgiou T, Morozov SV, Grigorenko AN, Geim AK, Casiraghi C, Castro Neto AH, Novoselov KS (2013) Strong light-matter interactions in heterostructures of atomically thin films. Science 340:1311–4
26. Klots AR, Newaz AKM, Wang B, Prasai D, Krzyzanowska H, Lin J, Caudel D, Ghimire NJ, Yan J, Ivanov BL, Velizhanin KA, Burger A, Mandrus DG, Tolk NH, Pantelides ST, Bolotin KI (2014) Probing excitonic states in suspended two-dimensional semiconductors by photocurrent spectroscopy. Sci Rep 4:6608